

## Structural, dielectric and magnetic properties of rare earth doped multiferroic $\text{Bi}_{0.90}\text{RE}_{0.10}\text{FeO}_3$ ceramics

Hemant Singh<sup>a</sup> and Manoj Baloni<sup>b\*</sup>

<sup>a</sup>Department of Physics, Government Post Graduate College, Rishikesh, Dehradun, India

<sup>b</sup>Department of Physics, SGRR P. G. College, Dehradun, India

\*Corresponding Author: Manoj Baloni<sup>b</sup>

Assistant Professor, Department of Physics  
SGRR P. G. College, Dehradun, India.

### Abstract

Polycrystalline  $\text{BiFeO}_3$  (BFO) and  $\text{Bi}_{0.90}\text{RE}_{0.10}\text{FeO}_3$  ( $\text{RE} = \text{Dy}, \text{Gd}, \text{Ho}$  and  $\text{La}$ ) ceramics have been synthesized by standard solid-state reaction method. The effect of rare earth doping on the structural, dielectric and magnetic properties of the  $\text{BiFeO}_3$  multiferroic perovskite was studied. X-ray diffraction pattern revealed that all the samples showed rhombohedral perovskite structure. In the vicinity of the antiferromagnetic Néel temperature ( $T_N$ ), an anomaly in the dielectric constant ( $\epsilon$ ) and dielectric loss ( $\tan(\delta)$ ) was observed. Magnetic hysteresis loops measured at 300K indicated weak ferromagnetism in  $\text{RE}^{3+}$  substituted  $\text{BiFeO}_3$  ceramics. The room temperature magnetic moment at 7T was found to increase with rare earth ions.

### Introduction

The coupling of minimum two of the possible ferroic orders viz., (anti)ferromagnetism, (anti)ferroelectric and (anti)ferroelastic leads to multiferroic materials [1]. This coupling of ferroelectricity and ferromagnetism lead to magnetoelectric effect and magnetodielectric effect as additional functionalities [2]. The multiferroic  $\text{BiFeO}_3$  (BFO) exhibits ferroelectricity and antiferromagnetic with weak ferromagnetism resulting from spin canting at room temperature.  $\text{BiFeO}_3$  possesses a rhombohedral distorted perovskite crystal structure with space group of  $R3c$  and a high Curie temperature ( $T_C \sim 1103$  K) and G-type canted antiferromagnetic order below a high Néel temperature ( $T_N \sim 643$  K) [3, 4]. An enhanced magnetization and a large polarization have been obtained in the heteroepitaxial constrained films [5]. Thus, multiferroic  $\text{BiFeO}_3$  is a promising material for application in storage devices [6-8].

However,  $\text{BiFeO}_3$  has some drawbacks for room temperature applications, such as large leakage current, (induced by defects, such as impurities, non-stoichiometry and oxygen vacancies), high dielectric loss and unsaturated magnetic loops. The major reason of the leakage current is generation of oxygen vacancies in  $\text{BiFeO}_3$ , which is mostly generated during the heat treatment. The partial substitution of  $\text{Fe}^{3+}$  site with higher-valence cations of  $\text{Ti}^{4+}$ ,  $\text{Zr}^{4+}$  has effectively decreased the leakage current [9,10] and several groups have reported partial substitution of  $\text{Bi}^{3+}$  with +3 valence cations of rare earth elements to improve the magnetic and ferroelectric properties of  $\text{BiFeO}_3$  [11-13]. In this study, we report the synthesis of  $\text{BiFeO}_3$  based ceramics doped by  $\text{RE}^{3+}$  for partial  $\text{Bi}^{3+}$ . The effect of rare earth substitution on structural, dielectric and magnetic properties of  $\text{BiFeO}_3$  based ceramics were investigated.

### Experimental

The rare earth doped  $\text{BiFeO}_3$  ceramic samples, namely  $\text{Bi}_{0.90}\text{RE}_{0.10}\text{FeO}_3$  (RE = Dy, Gd, Ho and La) were prepared by standard solid state reaction method. Stoichiometric ratios of  $\text{Bi}_2\text{O}_3$ ,  $\text{Fe}_2\text{O}_3$  and  $\text{RE}_2\text{O}_3$  were mixed and ground thoroughly in acetone medium to get homogeneous mixture and calcined at  $800^\circ\text{C}$  for 2 h. These calcined powders were then pressed into disks of thickness 1 mm and diameter 10 mm. The final sintering of the pellets was done at  $820^\circ\text{C}$  for 2 h. The pellets were silver pasted for dielectric measurements. The X-ray diffraction (XRD) pattern of the ceramics was recorded at room temperature using an X-ray powder diffractometer (Bruker D8 Advance) with  $\text{Cu } K\alpha$  radiation, in a Bragg angles range  $2\theta$  ( $20^\circ$ - $60^\circ$ ). To study the morphology of the samples field effect scanning electron microscopy (FESEM) was used. The dielectric measurements were done using an automated HIOKI 3532-50 Hi tester, LCR meter. Magnetization data were collected using a superconducting quantum interference device (SQUID).

### Results and discussion

Figure 1 shows the XRD patterns of  $\text{BiFeO}_3$  (BFO) and all the rare earth doped compositions. From the XRD analysis, it was observed that  $\text{Bi}_{0.90}\text{RE}_{0.10}\text{FeO}_3$  (RE = Dy, Gd, Ho and La) has the characteristic well crystallized rhombohedral pattern with the space group  $R3c$  as that of pure  $\text{BiFeO}_3$ . Some impurity peaks of  $\text{Bi}_{25}\text{FeO}_{39}$  and  $\text{Bi}_2\text{Fe}_4\text{O}_9$  were also observed for  $\text{BiFeO}_3$  (BFO) in the XRD data (marked by \* in Fig. 1). The existence of  $\text{Bi}_{25}\text{FeO}_{39}$  and  $\text{Bi}_2\text{Fe}_4\text{O}_9$  as impurity phases has been reported by several authors [14] due to narrow temperature range for the synthesis of BFO. The rare earth dopings suppressed the impurity peaks. It is seen in the patterns that with diffraction peaks slightly shifted to a high diffraction angle for Dy and no shifting for Ho and La doping samples. In Gd doped BFO ceramic sample, (104) and (110) peaks merge together to a single broad peak indicating a change from rhombohedral structure to pseudo-cubic structure. This might originate from the lattice distortion of the samples due to different rare earth ion contents, different ionic radii between  $\text{RE}^{3+}$  and  $\text{Bi}^{3+}$ . The equivalent hexagonal lattice parameters obtained from XRD patterns are  $a = 5.5700 \text{ \AA}$ ,  $c = 13.8126 \text{ \AA}$  for BFO,  $a = 5.5640 \text{ \AA}$ ,  $c = 13.8078 \text{ \AA}$  for Dy,  $a = 5.6146 \text{ \AA}$ ,  $c = 13.5390 \text{ \AA}$  for Gd,  $a = 5.5700 \text{ \AA}$ ,  $c = 13.8196 \text{ \AA}$  for Ho and  $a = 5.5700 \text{ \AA}$ ,  $c = 13.7771 \text{ \AA}$  for La doped BFO multiferroic ceramics.

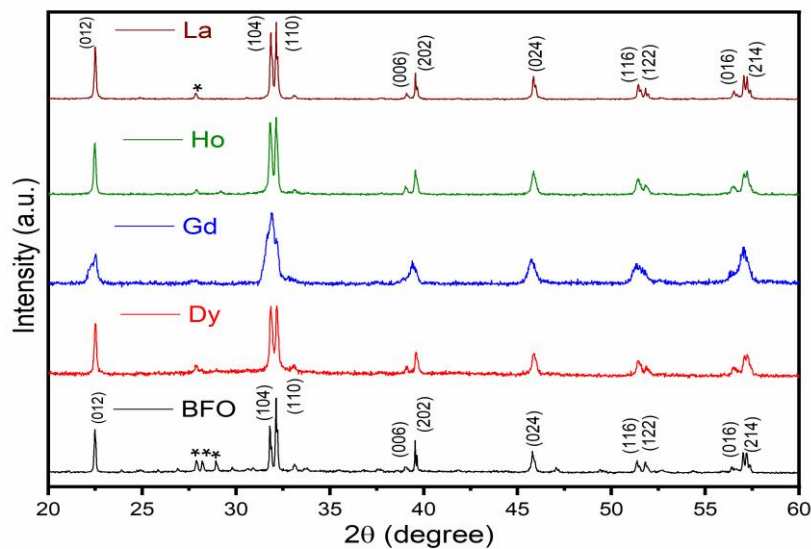


Figure 1. X-ray diffraction pattern of pure  $\text{BiFeO}_3$  and  $\text{Bi}_{0.90}\text{RE}_{0.10}\text{FeO}_3$  (RE = Dy, Gd, Ho and La). (\*) represent the  $\text{Bi}_{25}\text{FeO}_{39}$  and  $\text{Bi}_2\text{Fe}_4\text{O}_9$  impurity phases respectively.

Figure 2 shows the surface microstructures of BFO and rare earth (Dy, Gd, Ho and La) doped BFO ceramics. It is clear from the micrographs that well developed grains are observed and the observed grains are randomly oriented with a certain amount of intergranular porosity and distributed over the entire sample for the prepared BFO and rare earth doped samples.

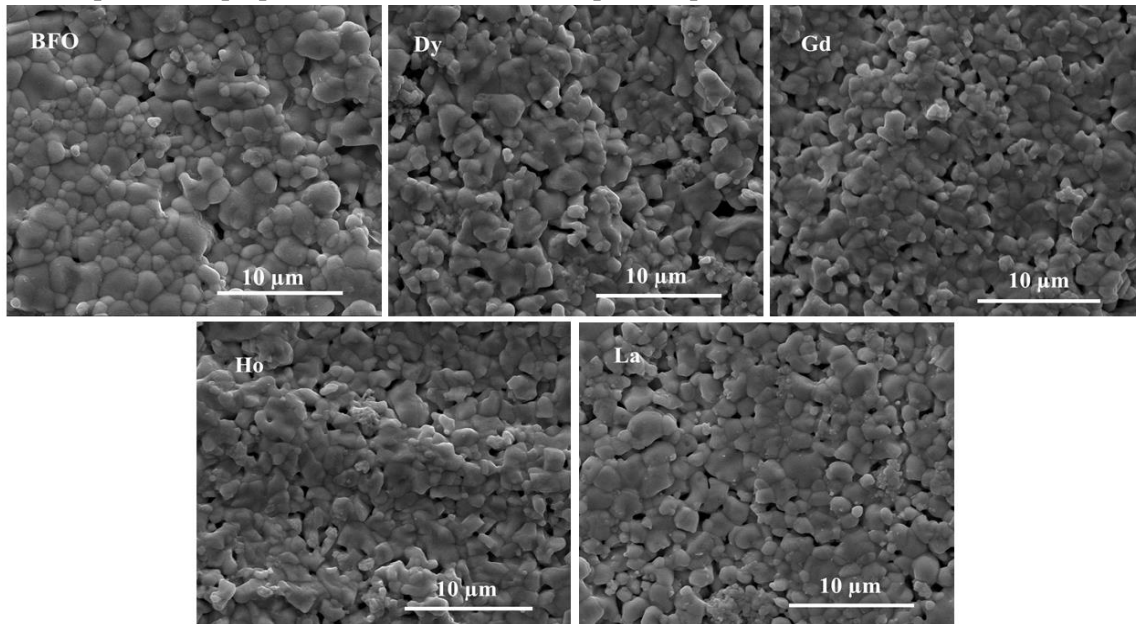


Figure 2. FESEM images of  $\text{BiFeO}_3$  and  $\text{Bi}_{0.90}\text{RE}_{0.10}\text{FeO}_3$  (RE = Dy, Gd, Ho and La).

Figure 3 shows the frequency dependence of dielectric constant and dielectric loss tangent of the prepared rare earth doped BFO ceramics. The dielectric constant decreases with the increase in frequency for all the prepared samples due to the inability of the electric dipoles to switch with the frequency of the applied electric field for high frequencies [15] and varies with the rare earth doping. The dielectric loss tangent is attributed to domain wall resonance. The dielectric loss tangent decreases with increase in frequency for pure BFO and rare earth doped samples and is low at higher frequencies due to the inhibition of domain wall motion.

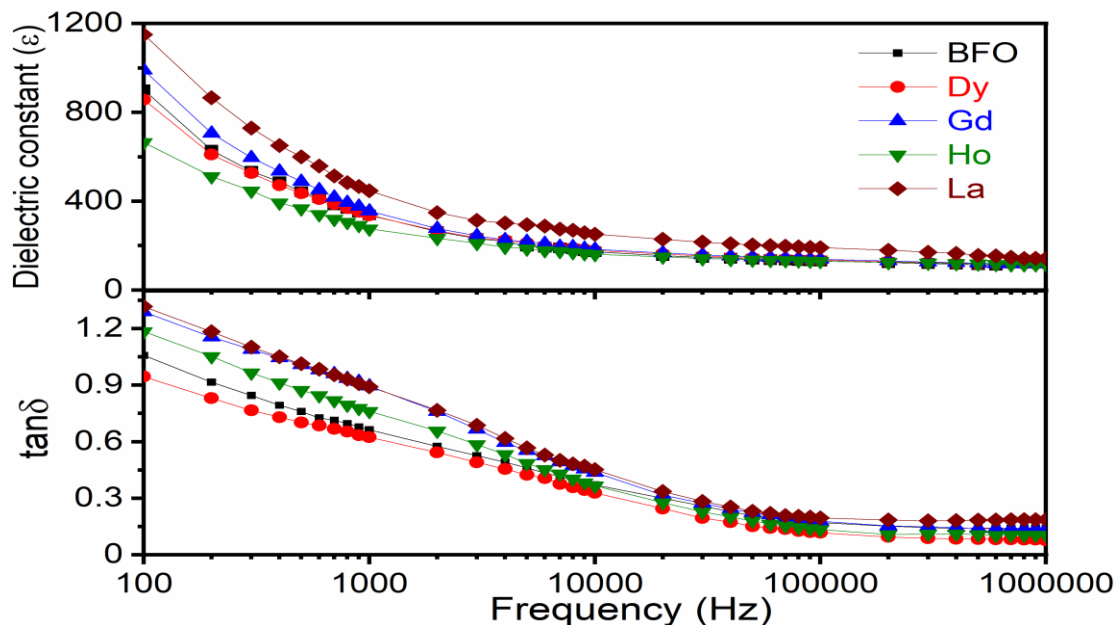


Figure 3. Frequency dependence of dielectric constant ( $\epsilon$ ) and dielectric loss tangent ( $\tan\delta$ ) of BFO and  $\text{Bi}_{0.90}\text{RE}_{0.10}\text{FeO}_3$  (RE = Dy, Gd, Ho and La).

The temperature dependence of dielectric constant ( $\epsilon$ ) and loss tangent ( $\tan\delta$ ) at 1MHz is shown in Fig. 4. A dielectric anomaly in dielectric constant has been observed in the vicinity of Néel temperature for BFO and all the rare earth doped ceramics in the  $\text{Bi}_{0.90}\text{RE}_{0.10}\text{FeO}_3$  system. The dielectric loss tangent was almost constant upto 300 °C and after that it increased sharply. The peaks in the dielectric constant patterns and increase in dielectric constant, obtained here may be attributed to change from one state of electric dipole ordering to another because of antiferromagnetic transitions/possible magnetoelectric coupling effect [16]. Similar kind of dielectric anomaly was also reported by several authors in the vicinity of Néel temperature [17]. The Landau–Devonshire theory of phase transitions predicated this type of dielectric anomaly in magnetoelectrically ordered systems as an effect of vanishing magnetic order on electric order [18]. Compared to  $\text{BiFeO}_3$ , the value of  $\tan\delta$  of all the  $\text{RE}^{3+}$  substituted ceramic samples remained smaller than that of  $\text{BiFeO}_3$  in the entire measured temperature range. This indicates that the oxygen vacancy in  $\text{BiFeO}_3$  was controlled by  $\text{RE}^{3+}$  doping and thereby improved its resistivity. The rise in the value of dielectric constant beyond the peaks with high value of  $\tan\delta$  observed in the corresponding temperature range may be due to the space charge polarization [17].

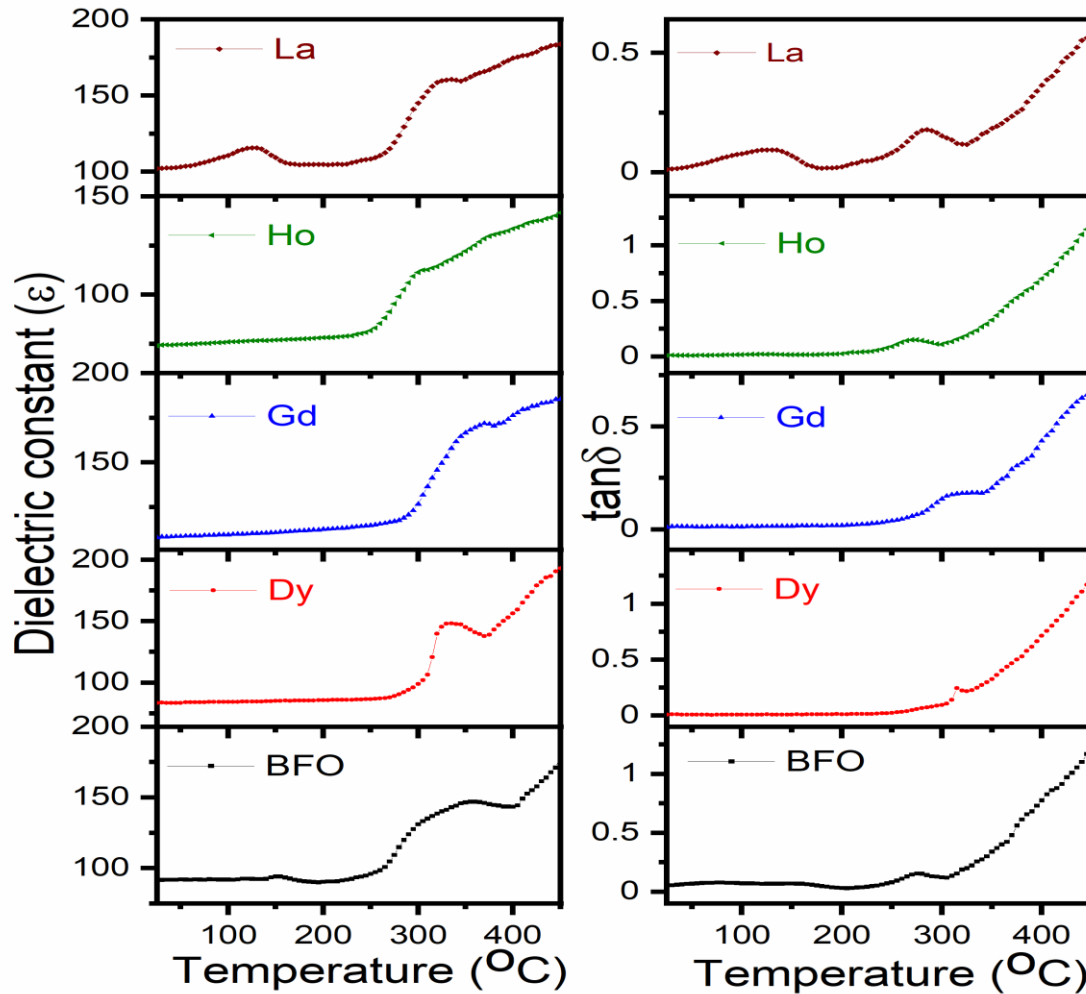


Figure 4. Temperature dependence of dielectric constant ( $\epsilon$ ) and dielectric loss tangent ( $\tan\delta$ ) of  $\text{BiFeO}_3$  (BFO) and  $\text{Bi}_{0.90}\text{RE}_{0.10}\text{FeO}_3$  (RE = Dy, Gd, Ho and La).

Figure 5 shows the magnetization hysteresis loops for pure BFO and rare earth (Dy, Gd, Ho and La) doped BFO ceramics at 300 K. The magnetization varies linearly with the applied magnetic field upto 7 T at 300 K for pure BFO sample. A similar magnetization character was also reported by other authors [18]. The magnetic structure of  $\text{BiFeO}_3$  was proved to be antiferromagnetic with the G-type spin ordering modulated by a cycloidal spiral with a large period  $\lambda=620\pm 20\text{\AA}$  below the Néel temperature [19, 20]. However, the  $\text{RE}^{3+}$  doped ceramics exhibited a ferromagnetic nature with magnetic hysteresis loops. The non-saturated MH loops upto 7 T exhibiting the basic antiferromagnetic nature of the samples. The appearance of hysteresis loop for  $\text{RE}^{3+}$  doped samples may be due to the canting of antiferromagnetically ordered Fe-O-Fe chain of spins resulting in the weak spontaneous magnetic moment. The change in the bond angle of Fe-O-Fe may be a result of distortion created by the  $\text{RE}^{3+}$  doping, changing the statistical distribution of  $\text{Fe}^{3+}/\text{Fe}^{2+}$  as a result of charge compensation. The non-attainability of saturation may be due to the uncompensated

antiferromagnetic nature persisting in the samples. The remnant magnetization for Dy is 0.0303, Gd is 1.229, Ho is 1.560 and La is 0.527 emu/g.

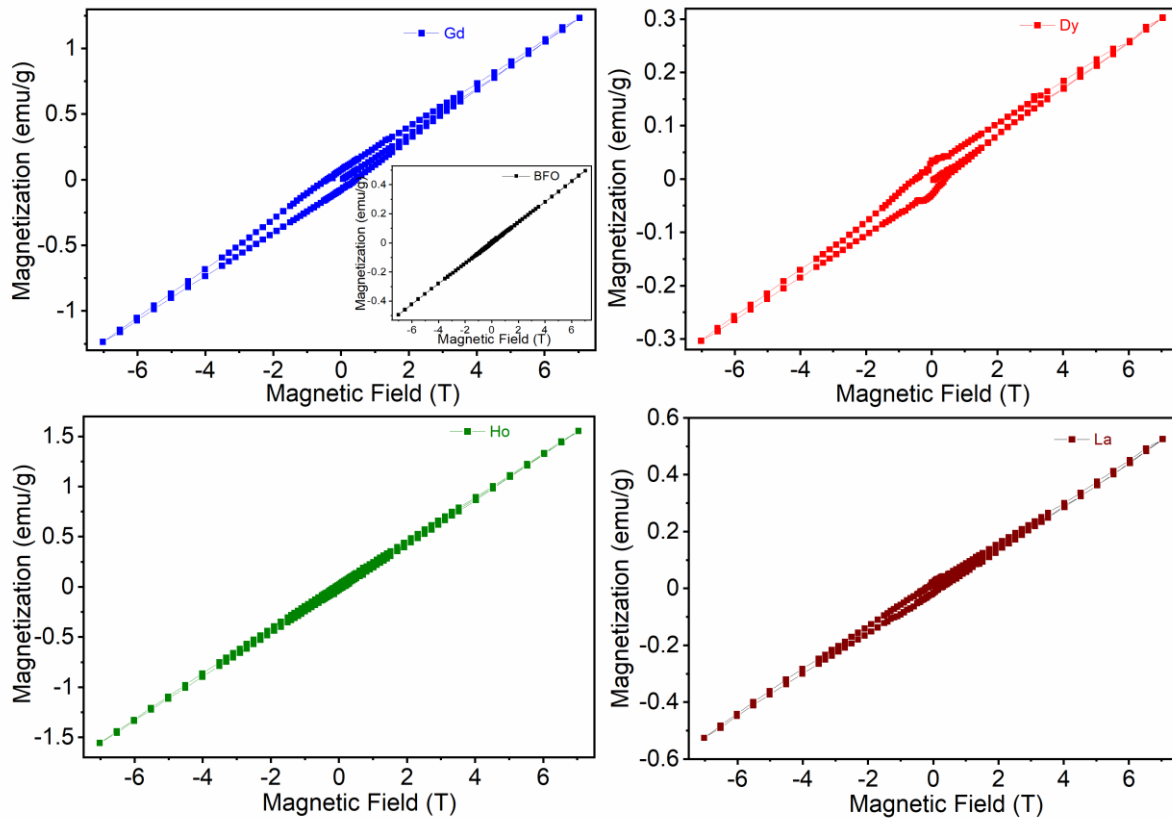


Figure 5. Room Temperature Magnetic hysteresis loops  $\text{BiFeO}_3$  and  $\text{Bi}_{0.90}\text{RE}_{0.10}\text{FeO}_3$  (RE = Dy, Gd, Ho and La).

## Conclusion

Pure BFO and  $\text{RE}^{3+}$  substituted BFO ceramics were synthesized using a solid state reaction method. It is shown that BFO and  $\text{Bi}_{0.90}\text{RE}_{0.10}\text{FeO}_3$  crystallizes in the rhombohedral crystal structure at room temperature with the space group  $R3c$ . Appearances of impurity peaks in BFO was suppressed with the rare earth doping in BFO. The lowering of dielectric loss tangent by  $\text{RE}^{3+}$  substitution in the measured temperature range suggesting the control of oxygen vacancy and improved resistivity. An anomaly was observed in the dielectric constant near the antiferromagnetic Néel temperature ( $T_N$ ). The dielectric anomaly may signify the magnetoelectric coupling between polarization and magnetization. The room temperature MH loops shows slight increase in the magnetic parameter  $M_r$  with  $\text{RE}^{3+}$  doping showing weak ferromagnetic order and maximum magnetization was observed for Ho doped BFO ceramics.

## References

1. M. Fiebig, J. Phys. D: Appl. Phys. 38 (2005) R123-R152.
2. N. A. Hill, J. Phys. Chem B 104 (2000) 6694-6709.
3. Z. X. Cheng, X. L. Wang, C. V. Kannan, K. Ozawa, H. Kimura, T. Nishida, S. J. Zhang S, and T. R. Shrout, Appl. Phys. Lett. 88 (2006) 132909.  
A. K. Pradhan, K. Zhang, D. Hunter, J. B. Dadson, G. B. Loutts, P. Bhattacharya et al., J. Appl. Phys. 97 (2005) 093903.
4. J. Wang et al., Science 299 (2003) 1719-1722.

5. M. Y. Li, M. Ning, Y. G. Ma, Q. B. Wu, and C. K. Ong, *J. Phys. D: Appl. Phys.* 40 (2007) 1603-1607.
6. W. Eerenstein, N. D. Mathur and J. F. Scott, *Nature* 442 (2006) 759-765.
7. G. W. Pabst, L. W. Matin, Y. H. Chu and R. Ramesh, *Appl. Phys. Lett.* 90 (2007) 072902
8. G. D. Hu, S. H. Fan, C. H. Yang and W. B. Wu, *Appl. Phys. Lett.* 92 (2008) 192905.
9. H. Liu, Z. Liu and K. Yao, *Physica B* 391 (2007) 103-107.
10. P. Uniyal and K. L. Yadav, *J. Phys.: Condens. Matter* 21 (2009) 012205.
11. K. S. Nalwa and A. Garg, *J. Appl. Phys.* 103 (2008) 044101.
12. P. Uniyal and K. L. Yadav, *J. Phys.: Condens. Matter* 21 (2009) 405901.
13. T. T. Carvalho and P. B. Tavares, *Mater. Lett.* 62 (2008) 3984.
14. M. Kumar and K. L. Yadav, *J. Phys.: Condens. Matter* 19(2007) 242202.
15. R. K. Mishra, D. K. Pradhan, R. N. P. Choudhary and A. Banerjee, *J. Magn. Magn. Mater.* 320 (2008) 2602-2607.
16. M. Kumar and K. L. Yadav, *J. Phys.: Condens. Matter* 18 (2006) L503-L508.
17. V. R. Palkar, D. C. Kundaliya, S. K. Malik, and S. Bhattacharya, *Phys. Rev. B* 69 (2004) 212102
18. I. Sosnowska and A. K. Zvezdin, *J. Magn. Magn. Mater.* 140 (1995) 167-168.
19. B. Ruetter, S. Zvyagin, A. P. Pyatakov, A. Bush, J. F. Li, V. I. Belotelov, A. K. Zvezdin and D. Viehland, *Phys. Rev. B* 69 (2004) 064114.